CrystEngComm



PAPER

View Article Online
View Journal | View Issue



Cite this: CrystEngComm, 2021, 23, 7479

SO₂ capture enhancement in NU-1000 by the incorporation of a ruthenium gallate organometallic complex†

Jorge García Ponce, ‡^a Mariana L. Díaz-Ramírez, (D) ‡^c Saidulu Gorla, chanaka Navarathna, (D) ‡^c Gabriela Sanchez-Lecuona, ‡^c Bruno Donnadieu, llich A. Ibarra (D) *^b and Virginia Montiel-Palma (D) *^c

The new material [RuGa]@NU-1000 incorporates Ru and Ga in 1.2 and 1.8 wt% respectively (molar ratio 1: 2). It stems from the grafting of the heterobimetallic ruthenium gallate complex, [MeRu(η^6 -C₆H₆)(PPh₃)₂][GaMe₂Cl₂] into the MOF material NU-1000. [RuGa]@NU-1000 shows enhanced adsorption of SO₂, specially at low pressures (10⁻³ bar) even when compared with other materials employing more expensive precious metals. Additionally, [RuGa]@NU-1000 samples need not be exposed to such harsh conditions for reactivation as they retain their adsorption properties after several cycles and preserve their porosity and structure. Thus, [RuGa]@NU-1000 is an excellent, selective material suitable for detection and precise quantification of SO₂, with a lower cost compared to other MOFs incorporating precious metals.

Received 12th August 2021, Accepted 8th October 2021

DOI: 10.1039/d1ce01076j

rsc.li/crystengcomm

Introduction

Once only produced by volcanic activity and wildfires, the daunting rise in the combustion of inefficiently processed fossil fuels containing sulfur compounds has now positioned our energy production processes as the main sources of hazardous sulfur dioxide in the atmosphere. A dramatic increase in the number of respiratory illnesses cases, and mortality, and more strict environmental regulations including the Clean Air Act, have prompted the development of efficient SO₂ detection methodologies, and cost-effective desulfurization strategies.

However, most current SO₂ capture techniques require harsh alkaline or acid conditions,⁷ are expensive to implement and are generally inefficient.⁸ Hence, the study and development of new adsorbent materials for efficient

SO₂ capture through physisorption processes are swiftly growing. 9-11 Zeolites, for instance, have been studied for

Coordination polymers (PCPs),¹⁷ have been studied over the last few years to undertake SO₂ adsorption.¹⁸ MOFs consist of organic linkers and metal ions or metal oxide clusters that produce one-, two-, or three-dimensional lattices depending on the linker and metal center composition.¹⁹ Properties such as adsorption capacity or selectivity in catalytic reactions can be finely customized by modifying the metal center, by adding new chemical functionalities to the linker,^{19–21} and even by incorporating additional metal sites by post-synthetic modifications of an existing MOF lattice, to synergically enhance the properties of the material.^{22–31}

In molecular chemistry, it is well known that SO_2 can bind the platinum group metals in several coordination modes, including η^1 -S or η^2 -S,O and even metastable η^1 -O, 32,33 either as a Lewis acid or base. 32,34 Not only that but the versatility of SO_2 coordination is also manifested in the facile thermal and photochemical interconversion of isomers. 35,36 Notable examples of reversible coordination of SO_2 to Ru(II), Ir(I), Ni(II), and $Pt(II)^{37,38}$ highlight the feasibility of their implementation in SO_2 removal applications. To make the systems economically suitable, the incorporation of additional precious metals in minimal quantities into the MOF is the target.

E-mail: argel@unam.mx

these possible applications. Yet, the regeneration processes entail considerable temperatures (>450 °C), therefore high costs and result in structural degradation with a net loss of porosity over time. Metal organic frameworks (MOFs), also named as porous.

Coordination polymers (PCPs), have been studied over

^a Escuela Moderna Americana, Cerro del Hombre 18, Romero de Terreros, Coyoacán, 04310, Ciudad de México, Mexico

b Laboratorio de Fisicoquímica y Reactividad de Superficies (LaFReS), Instituto de Investigaciones en Materiales, Universidad Nacional Autónoma de México, Circuito Exterior s/n, CU, Coyoacán, 04510, Ciudad de México, Mexico.

^c Department of Chemistry, Mississippi State University, Box 9573, Mississippi, 39762, USA. E-mail: vmontiel@chemistry.msstate.edu

 $[\]dagger$ Electronic supplementary information (ESI) available: Experimental section; full NMR and X-ray diffraction structure of complex [MeRu(η^6 -C₆H₆)(PPh₃)₂][GaMe₂Cl₂]. Adsorption isotherms of N₂ and SO₂; heat of adsorption of SO₂ and powder X-ray diffraction experiments. CCDC 2072598. For ESI and crystallographic data in CIF or other electronic format see DOI: 10.1039/d1ce01076i

[‡] These authors contributed equally to this work.

Herein, we report the incorporation of an organometallic compound of Ru and Ga into NU-1000 which gives rise to a new grafted MOF material with enhanced adsorption properties, principally at low pressures.

Results and discussion

Stimulated by our previous success on the incorporation of $[MeIr{\kappa^3(P,Si,Si)PhP(o-C_6H_4CH_2Si^1Pr_2)_2}]$ into zirconium based MOF mesoporous material NU-1000 (ref. 39) as a selective recyclable framework for SO₂ adsorption. 40 We now sought to extend this investigation to other metals. Post-synthetic modifications of NU-1000 to install well defined Co-Al, 28 Rh-Ga (ref. 29) or Ir (ref. 40) sites make use of the transition metal methyl complexes as precursors where the M-Me (M = Ir, Co, Rh) bond reacts with the OH/OH2 groups on the Zr nodes of NU-1000 presumably forming methane gas.^{28,29} We aimed at probing the reactivity when two different metals bearing a methyl substituent were reacted under similar conditions. Our group has been interested on the synthesis of transition metal/group 13 metal heterobimetallic complexes 41,42 towards catalytic and environmental applications. We proposed the heterobimetallic ruthenium gallate complex, $[MeRu(\eta^6-C_6H_6)(PPh_3)_2][GaMe_2Cl_2]$ (1) as an entry point to direct incorporation of two different metals into the MOF framework.

Complex 1 was synthesized through the room temperature reaction of [Ru(PPh₃)₃Cl₂] and excess GaMe₃ in benzene as solvent (ESI† eqn (S1)). After workup, complex 1 was isolated in good yield (69%) and fully characterized by spectroscopic methods both in solution and in the solid-state. Relevant NMR spectroscopic data include a triplet signal at δ 1.26 for the Ru bonded methyl hydrogens and a singlet signal at δ -0.20 for the methyl groups on Ga in the ¹H NMR spectrum. In the ¹³C{¹H} spectrum the methyl bonded to Ru appears at δ -17.0 as a triplet due to ^{31}P coupling while the methyl groups on Ga appear as a singlet at 0.34 ppm. Crystals suitable for X-ray diffraction analysis were grown from concentrated benzene/hexane solutions (Fig. 1). The solidstate structure closely resembles the reported aluminate analog bearing the same cation.43 The methyl Ru-C1 bond distance in 1 at 2.1559(14) Å is comparable though slightly longer than the corresponding in the aluminate analog at 2.124(9) Å. On the contrary, the Ru-P distances (Ru-P1 2.3703(4) and Ru-P2 2.3496(4)) are slightly shorter than in the Al complex (2.402(3) and 2.368(3) Å). Such differences can only be attributed to the different temperatures at which the measurements where performed, 203 K for the aluminate⁴³ we performed the measurement of complex 1 at 100 K.

A similar procedure to that previously mentioned 28,29,40 was employed for the grafting of complex 1 into the MOF material (Scheme S1, see ESI†). The color of the material changed from bright to pale yellow upon grafting of the Ru complex. To corroborate the formation of methane which had been previously proposed but to our knowledge not experimentally established. The Schlenk tube containing the

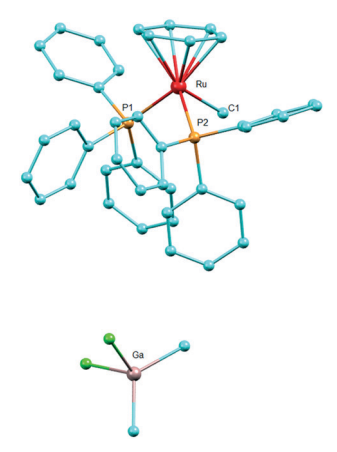
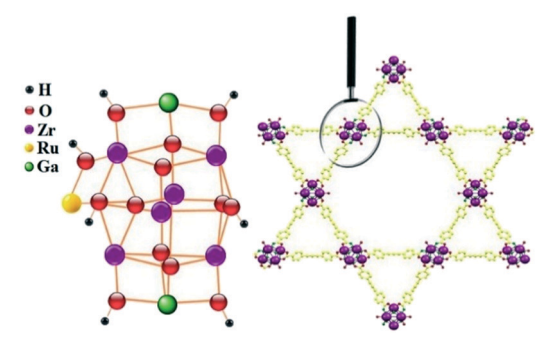


Fig. 1 Asymmetric unit view of the single crystal X-ray diffraction structure of complex 1. Thermal ellipsoids to 50% probability. All hydrogens are omitted for clarity as is the crystallized benzene solvent. Main bond distances (Å) and angles (°) are given here: Ru-C1 2.1559(14), Ru-P1 2.3703(4), Ru-P2 2.3496(4), Ru-C_{benzene} 2.2509(14)-2.3442(14). C1-Ru-P1 87.89(4), C1-Ru-P2 87.50(4), P1-Ru-P2 96.366(17).

reaction mixture was connected to an infrared gas cell and monitored. In the FTIR spectrum, the formation of methane gas was ascertained by its characteristic PQR pattern (see ESI,† Fig. S4).

After workup, PXRD analysis of the new material [RuGa] @NU-1000 confirmed the presence of the main features of parent NU-1000 and a BET surface area of 1796 m² g⁻¹ (see ESI,† Fig. S8b and S9a). LR-XPS analysis qualitatively confirmed the presence of Ga and small amounts of Ru. However, it should be noted that XPS is a surface sensitive method with the predominant contribution of the signals arising from the outer 10 Å region of the surface and may not represent the bulk composition. Furthermore, HR-XPS analyses of [RuGa]@NU-1000 showed the characteristic spectral patterns of Ga(2p), Ru(3d), Zr(3d) amongst other elements. More importantly, HR-XPS experiments show a binding energy shift to 1118.82 eV from 1117.91 eV for Ga(2p) and an increase of the atomic percentage of M-O or M-O-M linkages to 6.96% in comparison with that found in the unmodified material (2.73%, see ESI†). These data are consistent with the formation of Ga-O-Zr or Ru-O-Zr bonds.44,45 We carried out different determinations to interrogate the composition of the material including XPS, SEM-EDX and ICP-MS (see full details in ESI†). Most informatively, ICP-MS determinations on acid digested samples revealed ruthenium, gallium and zirconium contents of 1.78, 2.95 and 11.78 wt%, respectively. These values correspond to a molar ratio of 0.82 (Ru):1.96 (Ga) per Zr₆ unit (see ESI† for calculations) which can be approximated to 1 (Ru):2 (Ga):6 (Zr) as represented in Scheme 1. By SEM-EDX, a technique mostly focused on the surface analysis, we determine slightly lower values of Ru and Ga per Zr₆ cluster (0.7 Ru:1.2 Ga:6 Zr), as a consequence of the nature of the analysis. Yet, the ratio of Ga to Ru is still approximately of 2: 1, indicating a preference of the grafting of Ga over Ru in NU-1000.46,47

CrystEngComm **Paper**



Scheme 1 A representation of the Zr₆ node (left) of NU-1000 (right) grafted with complex 1 for the generation of material [RuGa]@NU-1000.

SO₂ adsorption-desorption isotherms were carried out using a Dynamic Gravimetric Gas/Vapor Sorption Analyzer, DVS vacuum (Surface Measurement Systems Ltd), from 0 to 1 bar at 298 K on the activated sample of [RuGa]@NU-1000 as shown in Fig. 2.

From the experimental adsorption isotherm at 298 K, a quick SO₂ uptake was recorded from 0.0 to approximately 0.01 bar with a total uptake of 0.5 mmol g⁻¹. Then, form 0.01 bar to around 0.1 bar, with a total uptake of approximately 2.2 mmol g⁻¹ was observed (Fig. 3, inset). From 0.1 to 0.35 bar, the adsorption isotherm showed an almost linear SO₂ uptake, with a maximum uptake of 5.6 mmol g⁻¹. Finally, from 0.35 to 1.0 bar (last value recorded from the experiment) the isotherm showed a slow increase in SO2 adsorption with a final value recorded of 7.5 mmol g⁻¹. Regarding the desorption isotherm, the almost complete release of SO₂ from the sample must be emphasized. Recent and ongoing SO₂ capture efforts call for those materials saturated with SO₂ to be heated or treated with additional chemicals to reuse them. In contrast, [RuGa]@NU-1000 samples need not be exposed to such harsh conditions; simple exposure to a vacuum at 298 K is enough to re-activate the material. A comparison of the isotherms at 298 K for NU-1000, [Ir]@NU-1000 and [Ru]@NU-1000 was plotted (Fig. 3) to show the effect of the metalation on SO₂ uptake. From 0.0 to around

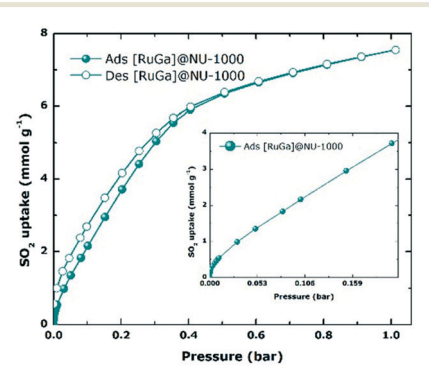


Fig. 2 Experimental SO₂ adsorption-desorption isotherm of [RuGa] @NU-1000 sample at 298 K and up to 1 bar (filled circles = adsorption; open circles = desorption). Inset: SO₂ adsorption isotherm from 0.0 to 0.21 bar.

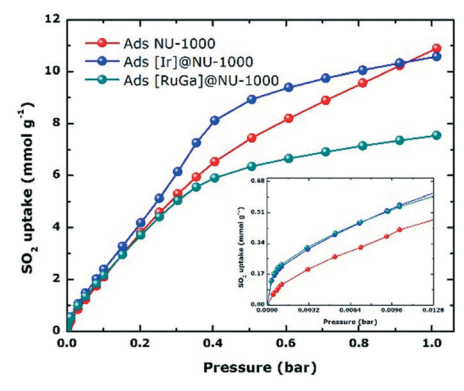


Fig. 3 Experimental SO₂ adsorption isotherms of NU-1000 (red), [Ir] @NU-1000 (blue), and [RuGa]@NU-1000 (green) samples at 298 K and up to 1 bar. Inset: SO₂ adsorption isotherms from 0.0 to 0.01 bar.

0.35 bar (the end of the region where SO₂ uptake resembles a linear function) all three materials present very similar behaviors, although [Ir]@NU-1000 has a clearly higher SO₂ uptake at higher pressures, further analysis reveals the opposite is true at low pressures. It is interesting to note however, that both materials grafted with organometallic complexes exhibit a very similar trend toward SO2: a shift from a steep linear SO2 uptake to a much less pronounced one as the, pressure exceeds 0.35 bar. Unmodified NU-1000, on the other hand, clearly deviates from this trend as its SO₂ uptake does not decrease nearly as much as the pressure surpasses the 0.35 bar threshold.

When we compared the isotherms for the three materials (Fig. 3, in-wet), [RuGa]@NU-1000 shows a higher SO₂ adsorption at low pressures. To further analyze this behavior, we plotted and fitted to a linear equation the adsorption values for all three materials (Fig. 4). This plot confirmed our hypothesis and provided a good approximation for the adsorption at low pressures: [RuGa]@NU-1000 has a significantly higher SO2 uptake than that of NU-1000 and compared to the previously reported [Ir]@NU-1000, the Ru/

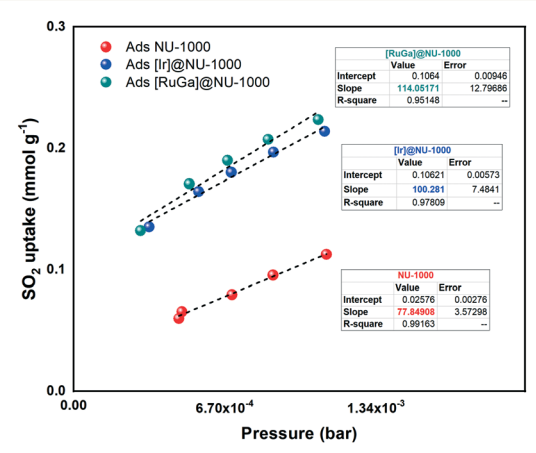


Fig. 4 Experimental SO₂ adsorption isotherms of NU-1000 (red), [Ir] @NU-1000 (blue), and [RuGa]@NU-1000 (green) samples at 298 K and up to approx. 0.001 bar. All three isotherms were fitted to the linear equations shown in the graph.

Ga-functionalized material exhibits a similar uptake. However, the affordability of ruthenium and gallium compared to that of iridium must also be noted: as of April 2021, iridium is approximately 10 times more expensive than ruthenium and around 400 times more expensive than gallium.49 Furthermore, our linear regressions show an increase in [RuGa]@NU-1000's sensibility (slope) towards small changes in SO₂ pressure compared to those of the other materials, showing a higher slope value (114 mmol g⁻¹ bar⁻¹) versus 100 and 77 mmol g⁻¹ bar⁻¹ for [Ir]@NU-1000 and NU-1000, respectively. PXRD analysis confirmed the retention of their crystal structure (see ESI,† Fig. S8c), after the first SO₂ sorption experiment. On a molecular level, this may be attributed to the availability of coordination sites in both Ga and Ru. The last one can easily undergo arene decoordination or hapticity change to allow SO₂ to bind.

Motivated by the high SO₂ adsorption at low pressures, we quantified the isosteric heat of adsorption (ΔH) at low coverage for fully activated [RuGa]@NU-1000. This value was estimated by fitting three adsorption isotherms at 298, 308, and 318 K to a Clausius-Clapeyron equation (see ESI,† Fig. S10 and Table S7). The average ΔH of [RuGa]@NU-1000 we calculated is of -104.7 kJ mol⁻¹. This ΔH suggests quite a strong interaction between SO₂ and the material, typical for SO_2 and open metal sites (e.g., KAUST-8, $\Delta H = -73.9$ kJ mol^{-1}).⁵⁰ Previous research has categorized ΔH values from -25 to -50 kJ mol⁻¹ as relatively week interactions mainly due to hydrogen bonding51 and has established these are useful for the capture of large amounts of gas,48 whereas values from -70 to -90 kJ mol⁻¹ are categorized as much stronger interactions and regarded ideal for detecting small amounts of SO_2 in the atmosphere (at ppm levels).⁵¹ The ΔH for [RuGa]@NU-1000 is characteristic then of a fairly strong interaction between the material and SO2, with a higher value than that reported for [Ir]@NU-1000 (-89.8 kJ mol⁻¹). Hence, [RuGa]@NU-1000 stands as a great candidate for SO_2 sensing even improving the SO₂ adsorption properties shown by [Ir] @NU-1000 as Fig. 4 illustrates.

As part of the characterization of the ruthenium material, we analyzed the SO_2 uptake retention by measuring the

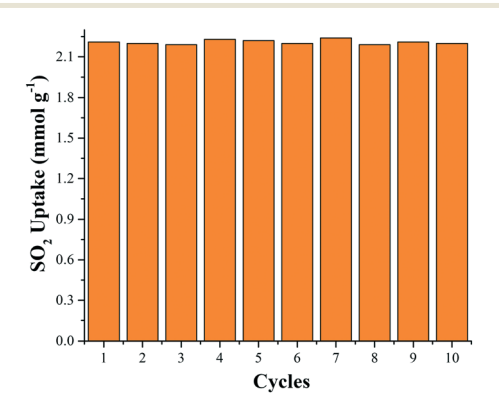


Fig. 5 Experimental maximum SO_2 uptake at 0.1 bar of a [RuGa]@NU-1000 sample at 298 K for each cycle.

maximum SO_2 uptake (from 0.0 to 0.1) bar at 298 K after ten adsorption–desorption cycles (Fig. 5) by simply applying vacuum (1.7 × 10^{-6} Torr) for 45 minutes at 298 K. The SO_2 uptake remained constant (2.2 mmol g^{-1}), which suggests that the sample was completely reactivated under the applied vacuum before the next adsorption–desorption cycle.

From our findings, it is clear that the SO_2 maximum uptake for [RuGa]@NU-1000 is not lost after ten cycles. PXRD analysis confirmed the retention of their crystal structure (see ESI,† Fig. S8d), after the cycling SO_2 sorption–desorption experiments.

While [RuGa]@NU-1000 showed a lower SO_2 uptake than those of NU-1000 and [Ir]@NU-1000 at relatively high pressures, its isosteric heat of adsorption shows a stronger interaction with SO_2 than that of [Ir]@NU-1000 and NU-1000 alone, posing it as a potentially more selective material towards this adsorbate. Furthermore [RuGa]@NU-1000 retains its porosity and adsorption capacity after several adsorption–desorption cycles, and it needs not be heated to high temperatures to reactivate the material, a vacuum at 298 K will suffice. These results contrast with other materials such as MOF-177 which shows remarkable SO_2 adsorption however, its zinc center interaction with the SO_2 molecules results in structural degradation and a loss of BET surface area over time. 52

Thus, the aforementioned characteristics position [RuGa] @NU-1000 as a promising candidate for SO₂ detection. Consequently, [RuGa]@NU-1000 stands not only as a better, more selective material suitable for detection and precise quantification of SO₂, but also as a lower cost alternative to [Ir]@NU-1000, making it a far more accessible and potentially useful technology in the SO₂ sensing niche.

Conclusions

Ruthenium gallate complex, [MeRu(η^6 -C₆H₆)(PPh₃)₂][GaMe₂-Cl₂], was successfully synthesized and characterised. The grafting of this complex into NU-1000 resulted in material [RuGa]@NU-1000, which drastically increases the material SO₂ affinity at pressures lower than 0.1 bar, while retaining the crystallinity of the material. A strong interaction between [RuGa]@NU-1000 and SO₂, identified by a high heat of adsorption (104.7 kJ mol⁻¹), would result in a more selective material towards this adsorbate. Materials such as this ruthenium gallate-functionalized MOF are key to developing new better and more efficient sensors to help stop and prevent further damage to the environment and human health by SO₂ pollution.

Conflicts of interest

There are no conflicts to declare.

Acknowledgements

We thank Ms. Niroshani S. Abeynayake for laboratory assistance with ICP-MS determinations and IR analysis. We

acknowledge financial support from start up funds of the Chemistry Department at Mississippi State University and NSF CHE-2102689. The authors would like to thank PAPIIT UNAM (IN202820), México for financial support.

Notes and references

- 1 J. N. Galloway, Acid deposition: Perspectives in time and space, Water, Air, Soil Pollut., 1995, 85, 15-24.
- 2 Z. Klimont, S. J. Smith and J. Cofala, The last decade of global anthropogenic sulfur dioxide: 2000-2011 emissions, Environ. Res. Lett., 2013, 8, 014003.
- 3 M. Matooane and R. Diab, Health risk assessment for sulfur dioxide pollution in South Durban, South Africa, Arch. Environ. Health, 2003, 58, 763-770.
- 4 P. Amoatey, H. Omidvarborna, M. S. Baawain and A. Al-Mamun, Emissions and exposure assessments of SOX, NOX, PM10/2.5 and trace metals from oil industries: A review study (2000-2018), Process Saf. Environ. Prot., 2019, 123, 215-228.
- 5 J. Schwartz and D. W. Dockery, Increased mortality in Philadelphia associated with daily air concentrations, Am. Rev. Respir. Dis., 1992, 145, 600-604.
- 6 The Clean Air Act, U. S. Environmental Protection Agency, U. S.Code Title 42. 1963, update 1990.
- 7 P. Córdoba, Status of Flue Gas Desulphurisation (FGD) systems from coal-fired power plants: Overview of the physic-chemical control processes of wet limestone FGDs, Fuel, 2015, 144, 274-286.
- 8 J. Y. Lee, T. C. Keener and Y. J. Yang, Potential flue gas impurities in carbon dioxide streams separated from coalfired power plants, J. Air Waste Manage. Assoc., 2009, 59, 725-732.
- 9 S. Furmaniak, A. P. Terzyk, P. A. Gauden, P. Kowalczyk and G. S. Szymański, Influence of activated carbon surface oxygen functionalities on SO2 physisorption - Simulation and experiment, Chem. Phys. Lett., 2013, 578, 85-91.
- 10 J. L. Llanos, A. E. Fertitta, E. S. Flores and E. J. Bottani, SO2 Physisorption on Exfoliated Graphite, J. Phys. Chem. B, 2003, 107, 8448-8453.
- 11 P. Zhang, H. Wanko and J. Ulrich, Adsorption of SO2 on Activated Carbon for Low Gas Concentrations, Chem. Eng. Technol., 2007, 30, 635-641.
- 12 B. E. Alver, M. Sakizci and E. Yörükoğullari, Adsorption of Sulphur Dioxide Using Natural and Modified Gördes Clinoptilolites, Adsorpt. Sci. Technol., 2011, 29, 413-422.
- 13 A. Srinivasan and M. W. Grutzeck, The Adsorption of SO2 by Zeolites Synthesized from Fly Ash, Environ. Sci. Technol., 1999, 33, 1464-1469.
- 14 I. Matito-Martos, A. Martin-Calvo, J. J. Gutiérrez-Sevillano, M. Haranczyk, M. Doblare, J. B. Parra, C. O. Ania and S. Calero, Zeolite screening for the separation of gas mixtures containing SO2, CO2 and CO, Phys. Chem. Chem. Phys., 2014, 16, 19884-19893.
- 15 A. J. Cramer and J. M. Cole, Removal or storage of environmental pollutants and alternative fuel sources with

- inorganic adsorbents via host-guest encapsulation, J. Mater. Chem. A, 2017, 5, 10746-10771.
- 16 N. D. Hutson, B. A. Reisner, R. T. Yang and B. H. Toby, Silver Ion-Exchanged Zeolites Y, X, and Low-Silica X: Observations of Thermally Induced Cation/Cluster Migration and the Resulting Effects on the Equilibrium Adsorption of Nitrogen, Chem. Mater., 2000, 12, 3020-3031.
- 17 R. F. Mendes and F. A. Almeida Paz, Transforming metalorganic frameworks into functional materials, Inorg. Chem. Front., 2015, 2, 495-509.
- 18 D. Britt, D. Tranchemontagne and O. M. Yaghi, Metalorganic frameworks with high capacity and selectivity for harmful gases, Proc. Natl. Acad. Sci. U. S. A., 2008, 105, 11623-11627.
- 19 O. M. Yaghi, G. Li and H. Li, Selective binding and removal of guests in a microporous metal-organic framework, Nature, 1995, 378, 703-706.
- 20 D. Yang, S. O. Odoh, T. C. Wang, O. K. Farha, J. T. Hupp, C. J. Cramer, L. Gagliardi and B. C. Gates, Metal-Organic Framework Nodes as Nearly Ideal Supports for Molecular NU-1000and UiO-66-Supported Iridium Catalysts: Complexes, J. Am. Chem. Soc., 2015, 137, 7391-7396.
- 21 D. Yang and B. C. Gates, Catalysis by Metal Organic Frameworks: Perspective and Suggestions for Future Research, ACS Catal., 2019, 9, 1779-1798.
- 22 J. Baek, B. Rungtaweevoranit, X. Pei, M. Park, S. C. Fakra, Y.-S. Liu, R. Matheu, S. A. Alshmimri, S. Alshehri, C. A. Trickett, G. A. Somorjai and O. M. Yaghi, Bioinspired Metal-Organic Framework Catalysts for Selective Methane Oxidation to Methanol, J. Am. Chem. Soc., 2018, 140, 18208-18216.
- Z. Li, A. W. Peters, V. Bernales, M. A. Ortuño, N. M. 23 Schweitzer, M. R. DeStefano, L. C. Gallington, A. E. Platero-Prats, K. W. Chapman, C. J. Cramer, L. Gagliardi, J. T. Hupp and O. K. Farha, Metal-Organic Framework Supported Cobalt Catalysts for the Oxidative Dehydrogenation of Propane at Low Temperature, ACS Cent. Sci., 2017, 3, 31-38.
- 24 Z. Li, N. M. Schweitzer, A. B. League, V. Bernales, A. W. Peters, A. B. Getsoian, T. C. Wang, J. T. Miller, A. Vjunov, J. L. Fulton, J. A. Lercher, C. J. Cramer, L. Gagliardi, J. T. Hupp and O. K. Farha, Sintering-Resistant Single-Site Nickel Catalyst Supported by Metal-Organic Framework, J. Am. Chem. Soc., 2016, 138, 1977-1982.
- 25 T. Ikuno, J. Zheng, A. Vjunov, M. Sanchez-Sanchez, M. A. Ortuño, D. R. Pahls, J. L. Fulton, D. M. Camaioni, Z. Li, D. Ray, B. L. Mehdi, N. D. Browning, O. K. Farha, J. T. Hupp, C. J. Cramer, L. Gagliardi and J. A. Lercher, Methane Oxidation to Methanol Catalyzed by Cu-Oxo Clusters Stabilized in NU-1000 Metal-Organic Framework, J. Am. Chem. Soc., 2017, 139, 10294-10301.
- 26 J. D. Evans, C. J. Sumby and C. J. Doonan, Post-synthetic metalation of metal-organic frameworks, Chem. Soc. Rev., 2014, 43, 5933-5951.
- 27 X. Zhang, Z. Huang, M. Ferrandon, D. Yang, L. Robison, P. Li, T. C. Wang, M. Delferro and O. K. Farha, Catalytic chemoselective functionalization of methane in a metalorganic framework, Nat. Catal., 2018, 1, 356-362.

Paper

28 A. B. Thompson, D. R. Pahls, V. Bernales, L. C. Gallington, C. D. Malonzo, T. Webber, S. J. Tereniak, T. C. Wang, S. P. Desai, Z. Li, I. S. Kim, L. Gagliardi, R. L. Penn, K. W. Chapman, A. Stein, O. K. Farha, J. T. Hupp, A. B. F. Martinson and C. C. Lu, Installing Heterobimetallic Cobalt–Aluminum Single Sites on a Metal Organic Framework Support, Chem. Mater., 2016, 28, 6753–6762.

- 29 S. P. Desai, J. Ye, J. Zheng, M. S. Ferrandon, T. E. Webber, A. E. Platero-Prats, J. Duan, P. Garcia-Holley, D. M. Camaioni, K. W. Chapman, M. Delferro, O. K. Farha, J. L. Fulton, L. Gagliardi, J. A. Lercher, R. L. Penn, A. Stein and C. C. Lu, Well-Defined Rhodium–Gallium Catalytic Sites in a Metal–Organic Framework: Promoter-Controlled Selectivity in Alkyne Semihydrogenation to E-Alkenes, *J. Am. Chem. Soc.*, 2018, 140, 15309–15318.
- 30 S. P. Desai, J. Ye, T. Islamoglu, O. K. Farha and C. C. Lu, Mechanistic Study on the Origin of the Trans Selectivity in Alkyne Semihydrogenation by a Heterobimetallic Rhodium– Gallium Catalyst in a Metal–Organic Framework, Organometallics, 2019, 38, 3466–3473.
- 31 S. P. Desai, C. D. Malonzo, T. Webber, J. Duan, A. B. Thompson, S. J. Tereniak, M. R. DeStefano, C. T. Buru, Z. Li, R. L. Penn, O. K. Farha, J. T. Hupp, A. Stein and C. C. Lu, Assembly of dicobalt and cobalt–aluminum oxide clusters on metal–organic framework and nanocast silica supports, *Faraday Discuss.*, 2017, 201, 287–302.
- 32 S. Aono and S. Sakaki, QM/MM Approach to Isomerization of Ruthenium(II) Sulfur Dioxide Complex in Crystal; Comparison with Solution and Gas Phases, *J. Phys. Chem. C*, 2018, 122, 20701–20716.
- 33 J. Li and A. Y. Rogachev, SO2 yet another two-faced ligand, *Phys. Chem. Chem. Phys.*, 2015, 17, 1987–2000.
- 34 A. V. Marchenko, A. N. Vedernikov, J. C. Huffman and K. G. Caulton, Evaluation of energies of isomeric SO2 complexes, *New J. Chem.*, 2003, 27, 680–683.
- 35 D. A. Johnson and V. C. Dew, Photochemical linkage isomerization in coordinated sulfur dioxide, *Inorg. Chem.*, 1979, **18**, 3273–3274.
- 36 X. Liu, X. Wang, B. Xu and L. Andrews, Spectroscopic observation of photo-induced metastable linkage isomers of coinage metal (Cu, Ag, Au) sulfur dioxide complexes, *Phys. Chem. Chem. Phys.*, 2014, 16, 2607–2620.
- 37 E. C. Moroni, R. A. Friedel and I. Wender, Solid state reversible reactions of square planar d8 complexes with sulfur dioxide, *J. Organomet. Chem.*, 1970, 21, P23–P27.
- 38 F. T. Esmadi and M. K. Fayyad, Reaction of sulfur dioxide with halocarbonyls of rhodium and iridium, *Synth. React. Inorg. Met.-Org. Chem.*, 1995, 25, 977–990.
- 39 T. C. Wang, N. A. Vermeulen, I. S. Kim, A. B. F. Martinson, J. F. Stoddart, J. T. Hupp and O. K. Farha, Scalable synthesis and post-modification of a mesoporous metal-organic framework called NU-1000, *Nat. Protoc.*, 2016, 11, 149.
- 40 S. Gorla, M. L. Díaz-Ramírez, N. S. Abeynayake, D. M. Kaphan, D. R. Williams, V. Martis, H. A. Lara-García, B. Donnadieu, N. Lopez, I. A. Ibarra and V. Montiel-Palma, Functionalized NU-1000 with an Iridium Organometallic

- Fragment: SO2 Capture Enhancement, ACS Appl. Mater. Interfaces, 2020, 12, 41758-41764.
- 41 C. J. Durango-García, J. O. C. Jiménez-Halla, M. López-Cardoso, V. Montiel-Palma, M. A. Muñoz-Hernández and G. Merino, On the nature of the transition metal-main group metal bond: synthesis and theoretical calculations on iridium gallyl complexes, *Dalton Trans.*, 2010, 39, 10588-10589.
- 42 C. J. Durango-Garcia, S. Jalife, J. L. Cabellos, S. H. Martinez, J. O. C. Jimenez-Halla, S. Pan, G. Merino and V. Montiel-Palma, Back to basics: identification of reaction intermediates in the mechanism of a classic ligand substitution reaction on Vaska's complex, *RSC Adv.*, 2016, 6, 3386–3392.
- 43 X. Fang, J. G. Watkin, B. L. Scott, K. D. John and G. J. Kubas, One-Pot Synthesis of (η6-Arene)bis(triphenylphosphine)(methyl)ruthenium(II) Cations. X-ray Structures of [(η6-C6H6)Ru(Me)(PPh3)2][AlCl2Me2] and the η5-Thiophene Analogue, Organometallics, 2002, 21, 2336–2339.
- 44 G. Schön, Auger and direct electron spectra in X-ray photoelectron studies of zinc, zinc oxide, gallium and gallium oxide, *J. Electron Spectrosc. Relat. Phenom.*, 1973, 2, 75–86.
- 45 J. Y. Shen, A. Adnot and S. Kaliaguine, An ESCA study of the interaction of oxygen with the surface of ruthenium, *Appl. Surf. Sci.*, 1991, 51, 47–60.
- 46 T. Islamoglu, K.-i. Otake, P. Li, C. T. Buru, A. W. Peters, I. Akpinar, S. J. Garibay and O. K. Farha, Revisiting the structural homogeneity of NU-1000, a Zr-based metal-organic framework, *CrystEngComm*, 2018, 20, 5913–5918.
- 47 From CCDC 1580411, the unit cell of NU-1000 considered as $C_{88}H_{44}O_{32}Zr_6$.
- 48 A. J. Hernández-Maldonado, R. T. Yang, D. Chinn and C. L. Munson, Partially Calcined Gismondine Type Silicoaluminophosphate SAPO-43: Isopropylamine Elimination and Separation of Carbon Dioxide, Hydrogen Sulfide, and Water, *Langmuir*, 2003, 19, 2193–2200.
- 49 https://www.dailymetalprice.com.
- 50 M. R. Tchalala, P. M. Bhatt, K. N. Chappanda, S. R. Tavares, K. Adil, Y. Belmabkhout, A. Shkurenko, A. Cadiau, N. Heymans, G. De Weireld, G. Maurin, K. N. Salama and M. Eddaoudi, Fluorinated MOF platform for selective removal and sensing of SO2 from flue gas and air, *Nat. Commun.*, 2019, 10, 1328.
- 51 E. Martínez-Ahumada, A. López-Olvera, V. Jancik, J. E. Sánchez-Bautista, E. González-Zamora, V. Martis, D. R. Williams and I. A. Ibarra, MOF Materials for the Capture of Highly Toxic H2S and SO2, *Organometallics*, 2020, 39, 883–915.
- 52 P. Brandt, A. Nuhnen, M. Lange, J. Möllmer, O. Weingart and C. Janiak, Metal-Organic Frameworks with Potential Application for SO2 Separation and Flue Gas Desulfurization, ACS Appl. Mater. Interfaces, 2019, 11, 17350-17358.